

OXYGEN AND MAGNESIUM ISOTOPIC COMPOSITIONS OF GROSSITE-BEARING INCLUSIONS IN DOM 08004 (CO3.1) AND DOM 08006 (CO3.0) CHONDRITES. S. B. Simon¹, A. N. Krot^{2*}, and K. Nagashima².

¹Department of the Geophysical Sciences, University of Chicago, Chicago, IL 60637, USA (sbs8@uchicago.edu).

²HIGP/SOEST, University of Hawai'i at Mānoa, Honolulu, HI 96821, USA (*sasha@higp.hawaii.edu).

Introduction: Ca,Al-rich inclusions (CAIs) in the least metamorphosed chondrites show a bimodal distribution of the initial $^{26}\text{Al}/^{27}\text{Al}$ ratio [$^{26}\text{Al}/^{27}\text{Al}_0$] with peaks at ~ 0 and $\sim 5 \times 10^{-5}$ [1–5], most likely indicating heterogeneous distribution of ^{26}Al in the protoplanetary disk during an apparently brief epoch of CAI formation [2]. Most CAIs in these chondrites are uniformly ^{16}O -rich ($\Delta^{17}\text{O} \sim -24\%$) suggesting formation in a gas of \sim solar composition [3,4]. The important exceptions are isotopically anomalous ^{26}Al -poor CAIs with fractionation and unidentified nuclear effects (FUN) [5], ^{26}Al -poor platy hibonite crystals (PLACs) [6], and ^{26}Al -poor grossite-rich CAIs in CH chondrites showing a range of $\Delta^{17}\text{O}$, from $\sim -35\%$ to $\sim -10\%$ [7,8]. Grossite, CaAl_4O_7 , is one of the most refractory minerals predicted to condense from a cooling gas of solar composition [9]. Grossite-bearing inclusions are a relatively rare type of CAIs in most chondrite groups, except CH chondrites, the only group where they have been extensively studied [10–13]. Here, we report on the mineralogy, petrography, O and Al-Mg isotope systematics of six grossite-bearing CAIs in DOM 08004 (CO3.1 [14]) measured *in situ* with the UH Cameca ims-1280. For analytical conditions during SIMS measurements see [12]. Isotopic compositions of grossite-bearing CAIs in DOM 08006 (CO3.0) will be reported at the meeting.

Mineralogy and Petrography: For details, see [14].

DOM 08004: CAI 16-1 has a hibonite (in wt%: ~ 0.9 MgO, ~ 1.9 TiO₂)–grossite–perovskite core surrounded by the layers of spinel, melilite (Åk_{1-18}), Al-diopside (0.6 – 9.6 Al₂O₃, 0 – 1 TiO₂), and forsterite (Fig. 1a). CAI 26-1 consists of platy hibonite (~ 0.7 MgO, ~ 1.6 TiO₂) crystals surrounded by grossite (Fig. 1b). CAIs 44-2 (Fig. 2a), 75-1 and 77-1 consist of several mineralogically-zoned bodies composed of grossite and perovskite, and surrounded by layers of spinel and melilite (Åk_{1-12}). CAI 55-1 occurs inside a magnesian porphyritic olivine-pyroxene chondrule (Fig. 2b). Its core consists of grossite, melilite (Åk_{3-11}), and perovskite; it is surrounded by layers of spinel+perovskite and plagioclase (Fig. 1f). The spinel layer is corroded by plagioclase and overgrown by Cr-bearing spinel. Grossite in all CAIs experienced incipient replacement by a secondary Fe-rich phase (“sec” in Figs. 1, 2).

DOM 08006: CAI 31-2 has a core composed of hibonite (~ 0.9 MgO, ~ 1.8 TiO₂), grossite, and perovskite; it is surrounded by the layers of melilite (Åk_{2-44}), Ti-free diopside (~ 0.2 Al₂O₃), forsterite (Fa₁) + FeNi-metal (oxidized to magnetite), and low-Ca pyroxene (Fs₁Wo_{0.1}) (Fig. 3a). CAI 56-1 has a corundum–hibonite (~ 0.6 MgO, ~ 1.1 TiO₂)–grossite core surrounded by the melilite (Åk_{11}) and Al-diopside rims. Corundum and hibonite are corroded by hibonite and grossite, respectively. CAI 99-1

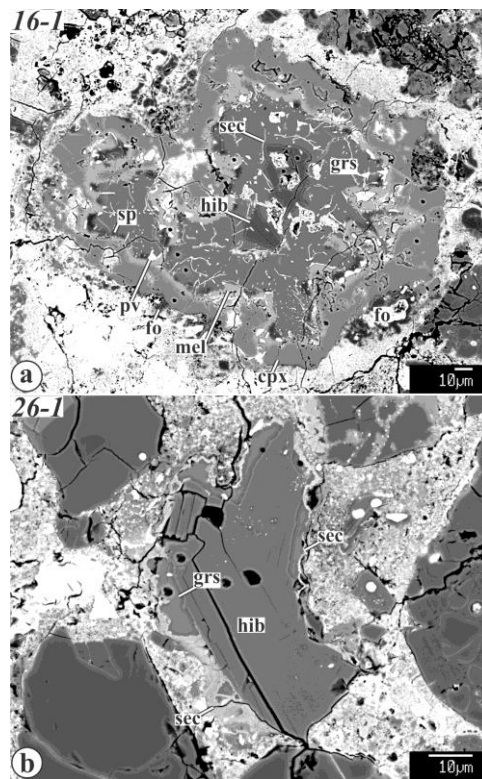


Fig. 1. BSE images of the ^{26}Al -poor grossite-bearing CAIs 16-1 and 26-1 from DOM 08004 (CO3.1). Hereafter: cor = corundum; cpx = high-Ca pyroxene; grs = grossite; hib = hibonite; mel = melilite; pv = perovskite; px = low-Ca pyroxene; sec = secondary phase; sp = spinel.

is an aggregate of several concentrically-zoned objects having spinel–hibonite (~ 2 MgO, ~ 5 TiO₂)–perovskite or grossite cores which are surrounded by the layers of melilite (Åk_2) and spinel–melilite (Åk_2), respectively (Fig. 3c).

Diverse secondary minerals (magnetite, N-rich metal, Ni-bearing sulfides, Fe,Ni-carbides, phyllosilicates, and fayalite) are observed in matrices and chondrules of DOM 08004 and DOM 08006, suggesting that both meteorites experienced hydrothermal alteration [15].

Oxygen isotopes: On a three-isotope oxygen diagram ($\delta^{17}\text{O}$ vs. $\delta^{18}\text{O}$), compositions of the grossite-bearing CAIs in DOM 08004 plot along \sim slope-1 line. In Fig. 4, we show $\Delta^{17}\text{O}$ values ($= \delta^{17}\text{O} - 0.52 \times \delta^{18}\text{O}$) of individual minerals in these CAIs. All CAIs are isotopically heterogeneous, with grossite and, in most cases, melilite being ^{16}O -depleted relative to spinel, hibonite, and Al,Ti-diopside. Spinel in the relict CAI 51-1 shows a range of $\Delta^{17}\text{O}$ most likely reflecting partial melting and overgrowth by Cr-bearing spinel during crystallization of the ^{16}O -poor host chondrule.

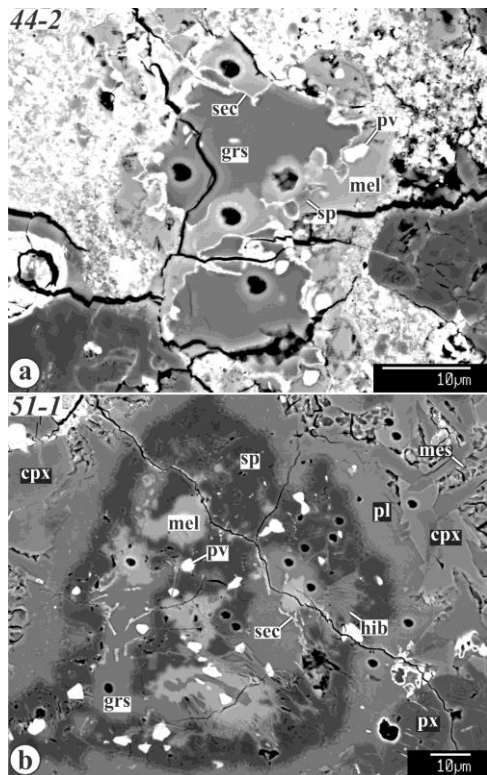


Fig. 2. BSE images of the ²⁶Al-rich grossite-bearing CAIs 44-2 and 51-1 from DOM 08004 (CO3.1).

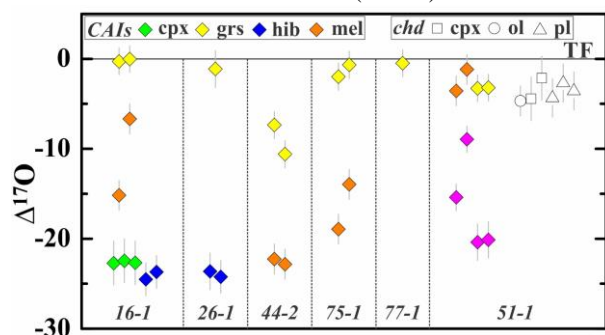


Fig. 4. $\Delta^{17}\text{O}$ values of the DOM 08004 grossite-bearing CAIs. TF = terrestrial fractionation line.

Magnesium isotopes: Hibonite and grossite in CAIs 16-1 and 26-1 show no resolvable excesses of ²⁶Mg*, (²⁶Al/²⁷Al)₀ < 5.7 × 10⁻⁷ and < 6.8 × 10⁻⁷, respectively. Grossite in CAIs 44-2, 51-1, 75-1 and 77-1 shows large ²⁶Mg* excesses correlated with their Al/Mg ratios, corresponding to inferred (²⁶Al/²⁷Al)₀ of (4.4 ± 0.3) × 10⁻⁵, (4.0 ± 0.3) × 10⁻⁵, (4.5 ± 0.3) × 10⁻⁵ and (4.3 ± 0.3) × 10⁻⁵, respectively. The (²⁶Al/²⁷Al)₀ values systematically lower than the canonical ratio are probably due to use of an improper Al/Mg sensitivity factor for grossite, that was assumed to be the same as for hibonite [3].

Discussion: The ¹⁶O-depleted compositions of grossite and melilite in DOM 08004 CAIs may have resulted from postcrystallization exchange during fluid-rock interaction on the CO chondrite parent body [15]. The alteration appears to not have affected the Al-Mg systematics

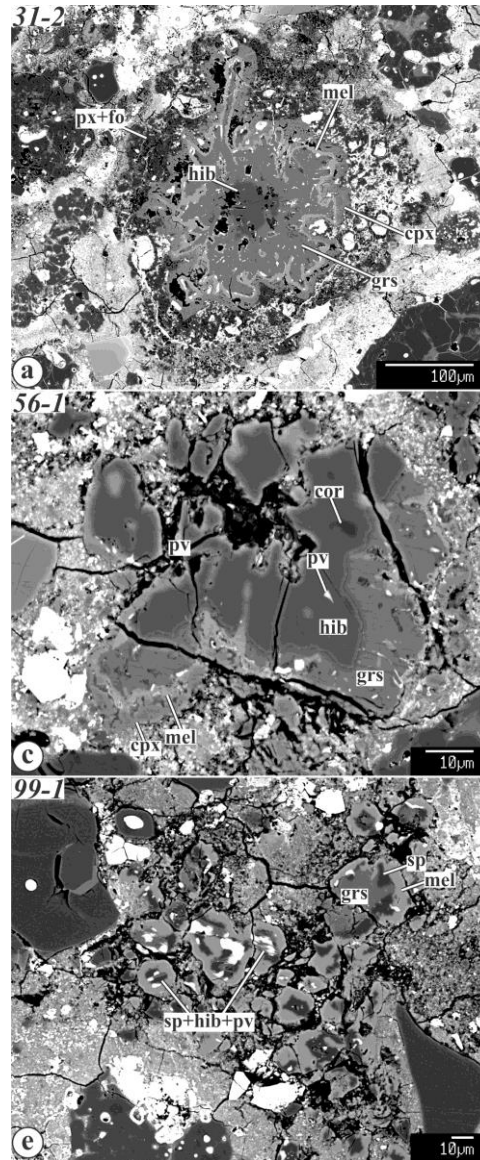


Fig. 3. BSE of the grossite-bearing CAIs 32-1, 56-1, and 99-1 from DOM 08006 (CO3.0).

of the CAIs. Therefore, the inferred (²⁶Al/²⁷Al)₀ likely reflect the heterogeneous distribution of ²⁶Al in the CAI-forming region. The ²⁶Al-poor CAIs could have formed prior to addition of ²⁶Al to the protoplanetary disk.

References: [1] MacPherson G. et al. (2014) *LPS*, 45, #2134. [2] Krot A. et al. (2012) *MAPS*, 47, 1948–1979. [3] Makide K. et al. (2009) *GCA*, 73, 5018–5051. [4] Kööp L. et al. (2016) *GCA*, 184, 151–172. [5] Krot A. et al. (2010) *ApJ*, 713, 1159–1166. [6] Kööp L. et al. (2016) *GCA*, 189, 70–95. [7] Krot A. et al. (2008) *ApJ*, 672, 713–721. [8] Gounelle M. et al. (2009) *ApJ*, 698, L18–L22. [9] Grossman L. (2010) *MAPS*, 45, 7–20. [10] Kimura M. et al. (1993) *GCA*, 57, 2329–2359. [11] Weber D. et al. (1995) *GCA*, 59, 803–823 [12] Krot A. et al. (2017a) *GCA*, in press. [13] Krot A. et al. (2016) *LPS*, 47, #1203. [14] Simon S. & Grossman L. (2015) *MAPS*, 50, 1032–1049. [15] Krot A. et al. (2017) *LPS*, 48, this issue.